



# An experimental investigation of a mass exchanger for transferring water vapor and inhibiting the transfer of other gases

E.M. Sparrow<sup>a,\*</sup>, J.P. Abraham<sup>a</sup>, G.P. Martin<sup>b</sup>, J.C.Y. Tong<sup>b</sup>

<sup>a</sup> Department of Mechanical Engineering, University of Minnesota, Minneapolis, MN 55455, USA

<sup>b</sup> XeteX Inc., 3530 East 28th Street, Minneapolis, MN 55406, USA

Received 25 November 2000; received in revised form 10 January 2001

## Abstract

A definitive experimental investigation has been performed to determine the transfer characteristics of a new type of mass exchanger. The exchanger was designed to perform the dual functions of transferring water vapor across its walls with a high degree of effectiveness while preventing the transport of other gaseous species. The heart of the exchanger is a novel permeable material synthesized by depositing an extremely thin polymer film atop a sheet of a common mass transferring polymer substrate. It was demonstrated that the synthesized composite-membrane sheets could be fashioned into modules and stacked to form a cross-flow mass exchanger. Two sets of experiments were performed to investigate the mass transfer characteristics of the exchanger for water vapor transfer. The first set of experiments was performed in a special highly and precisely instrumented, dual-stream, wind-tunnel test facility. On the other hand, the second set of experiments was carried out as a simulated field test. The results of these experiments revealed that mass transfer effectivenesses for water vapor as high as 50% could be readily obtained. To investigate the capabilities of the composite membrane to block the transfer of gaseous species other than water vapor, special experiments involving carbon dioxide were performed. These experiments decisively demonstrated that virtually no CO<sub>2</sub> could pass through the composite-membrane wall. The selectivity, which is the ratio of the effectiveness for water vapor transfer to the effectiveness of CO<sub>2</sub> transfer, was found to lie in the range between 21 and 61. © 2001 Published by Elsevier Science Ltd.

## 1. Introduction

The use of air-to-air heat exchangers is commonplace as an energy conservation modality in most climate-control devices. The energy savings result from the collection of what would otherwise be waste heat and the transferring of this heat to a second airstream which would otherwise have to be heated. Although not as commonly employed in current practice, the collection or extraction of moisture also presents a major opportunity for energy conservation. For instance, under summertime operating conditions, fresh, albeit humid

air taken from the outdoors may be passed into an indoor space with its humidity level intact. The reduction in humidity, appropriate to the attainment of human comfort, would normally be achieved by means of a refrigeration device (dehumidifier or air conditioner). The energy required to operate the refrigeration device can be saved if the incoming air were to be routed through a mass exchanger. Indeed, the mass exchanger can be combined with a heat exchanger to yield a single unit.

The focus of this paper is to describe the design, fabrication, and operating performance of a plate-type mass exchanger whose primary function is to facilitate the passage of water vapor between an airstream of higher humidity and a second airstream of lower humidity. A second function of the mass exchanger is to selectively block the transfer of the other gaseous species

\* Corresponding author. Tel.: +1-612-625-5502; fax: +1-612-624-1398.

E-mail address: esparrow@tc.umn.edu (E.M. Sparrow).

Nomenclature			
$A$	transfer area	$\varepsilon_{em}$	mass transfer effectiveness for water vapor, Eq. (1)
NTU	number of thermal transfer units, Eq. (4)	$\dot{m}$	mass flowrate
NTU <sub>m</sub>	number of mass transfer units, Eq. (6)	$\dot{m}_a$	mass flowrate of air
$R$	heat transfer resistance	$\omega$	humidity ratio
$R_1, R_2$	convective mass transfer resistances	<i>Subscripts</i>	
$R_d$	wall mass transfer resistance	CO <sub>2</sub>	carbon dioxide
$R_m$	total mass transfer resistance	MAX	largest quantity
$S$	selectivity, Eq. (8)	MIN	smallest quantity
$T$	temperature	EXH	exhaust stream
$U$	overall heat transfer coefficient	OUT	outside stream
$c_p$	specific heat	RET	return stream
$\varepsilon$	heat exchanger effectiveness, Eq. (3)	SUP	supply stream

between the airstreams. This concern with the blockage of gases other than water vapor stems from the current interest in indoor air quality. In public buildings and in many private residences, the issue of indoor air quality is of great importance and is being given considerable attention both among HVAC professionals and in the community at large. Indeed, the exchange of outdoor air, considered to be “fresh” air, is commonplace and suggests that the issue of indoor air quality is now regarded as being more critical than outdoor air quality.

Currently, there is limited commercial use of plate-type mass exchangers and very little in the published research literature. To the best knowledge of the authors, the research literature consists of a pair of papers by Fisk et al. [1,2] which are concerned with a mass exchanger in which the permeable material is paper. It was found that under cold-weather operation, the freezing of water caused significant damage to the paper. Other literature, Barringer and McGugan [3], has addressed the impact of mass exchangers on HVAC issues.

In the present paper, an altogether different type of permeable material is used to facilitate the exchange of water vapor between two flowing airstreams. The polymer is one commonly encountered in engineering practice. A special feature of the permeable material is the affixing of an extremely thin coating of another polymer whose function is to totally block the passage of gases other than water vapor through the mass exchanger walls. The function of the coating is to provide a property called selectivity. This issue will be discussed at greater length shortly.

In the presentation that follows, attention will first be focused on the physical issues of the mass exchanger and on the characteristics of its permeable walls. Subsequently, a brief description will be given of the special wind-tunnel facility that was used to evaluate the water vapor transfer characteristics and the selectivity characteristics of the tested mass exchanger. After this, the

experiments that were performed will be described. Finally, the experimental results will be presented along with a discussion of the practical implications of these results. A method will be developed and implemented for extending the range of parameters for which the experimental results can be applied.

## 2. The mass exchanger

A mass exchanger, in common with a recuperative heat exchanger, is a device whose function is to transfer a specific quantity between two flowing airstreams without direct mixing of the participating streams. In the recuperative heat exchanger, the quantity of interest is thermal energy; in a mass exchanger, water vapor is normally the desired transferred quantity. The main structural difference between a heat and mass exchanger is that in the former, the walls that separate the airstreams are impermeable to all fluids, whereas in the latter, these walls are permeable to water vapor. This definition of a mass exchanger represents a vision that is often not fulfilled because most permeable materials permit the passage of a number of gaseous species. It is only when special coatings are applied that the walls become selective. To the knowledge of the authors, all commercially available mass exchangers are not selective and pass a variety of gases through their walls.

A schematic diagram of the mass exchanger that was designed and fabricated as part of this investigation is shown in Fig. 1. As seen there, the exchanger consists of a stack of rectangular ducts, with every other duct in the stack oriented at 90° to its neighbors. Careful observation of Fig. 1 reveals that one family of stacked channels contains a corrugated spacer in each of its ducts, whereas in the second family of channels, the individual ducts are free of any obstruction. The utilization of fully open passages facilitates the drainage of condensate in

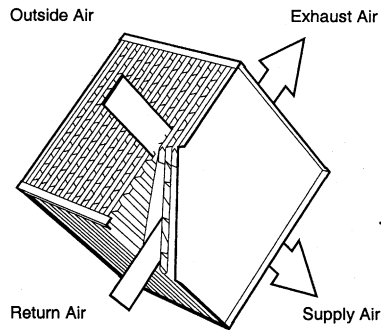


Fig. 1. Plate-type, cross-flow mass exchanger.

the event that the exchanger was to be operated at temperatures sufficiently low to cause condensation of the vapor.

The mass exchanger differs fundamentally from its counterpart heat exchanger in that the walls which separate neighboring channels are not made of an impermeable material such as aluminum. Rather, a wall consists of a polymer sheet that is stretched tightly across one of the faces of a corrugated spacing plate and bonded to it at each of the successive peaks of this plate. A second polymer sheet is similarly bonded to the other face of the corrugated spacing plate. This construction creates a sandwich-like module with the polymer sheets corresponding to the bread and the corrugated plate to the filling. In the assembly of the mass exchanger, the individual modules were stacked one on top of the other with spacer bars interposed at the ends in order to separate the respective neighboring modules. The spacer bars were sealed to the adjacent surfaces of the module to prevent leaks between the airstreams. The presence of the spacer bars created the array of open channels.

The stacking operation was performed in a frame that consisted of horizontal top and bottom surfaces and vertical members that formed the edges of the assembly. Sealant was applied at all locations where leaks might have occurred. Subsequent to the final assembly, weights were placed atop the stack for the purpose of compression. Once the compression was achieved, rivets were applied to buttress the exchanger, and the weights were removed.

The application of the thin polymer coating that facilitated selective passage of the water vapor was a painstaking process which was performed utilizing a continuous web-like processing machine. The underlying substrate (also a polymer, as noted above) arrived in roll form, and its unrolling served as the initial point of the moving web. As the web progressed, it was subjected to a number of chemical processes that served both to create and to cure the ultra-thin film to ensure its permanence. The long sheet of coated polymer was then cut

into shorter lengths and fixed to the faces of the corrugated spacer plates as already discussed.

The presence of the thin polymer film presented a hole-free surface to the airstream passing over it. The absence of holes prevented passage of other gases besides water vapor through the composite membrane formed by the substrate and film. Passage of the water vapor occurs by a process called solution-diffusion. Water vapor is soluble in the polymer that forms the thin-film coating of the composite membrane. The dissolved water vapor is driven across the film by the difference in partial pressure existing between the surfaces of the film. Once the dissolved vapor has passed across the film, it encounters the substrate that is porous to water vapor and other gases. The vapor traverses the substrate and then exits into the less-humid airstream.

The dimensions of each face of the mass exchanger are  $13 \frac{7}{8}$  by  $10 \frac{3}{4}$  in. (35.2 by 27.3 cm), and the lengths of all flow passages are  $12 \frac{1}{4}$  in. (31.1 cm). Of the 101 channels that comprise the mass exchanger, 51 are of the open type and 50 include the corrugated spacers. All the channels are of  $\frac{1}{8}$ -in. (0.318-cm) height. The corrugated spacers were made of 0.042-in. (0.11-cm) thick aluminum sheet stock that was fashioned by a corrugating machine to have a wavelength of  $\frac{11}{32}$  in. (0.873 cm) and a height of  $\frac{1}{8}$  in. (0.381 cm). The corrugating machine created triangular-shaped passages with sharp vertices. The overall thickness of the sandwich-like module that consisted of two layers of the composite membrane, the corrugated spacer plate, and the adhesive, which anchors the membrane to the corrugations, is approximately 0.15 in. (0.38 cm).

To facilitate the attainment of air velocities in the mass exchanger passages to a practical range with the available air-handling equipment, it was necessary to reduce the aforementioned exchanger face area. This was accomplished by masking off 20 of the 50 modules, leaving 30 open channels in each of the flow directions.

### 3. The test facility

In order to enable definitive characterization of the mass exchanger that was designed and fabricated, as previously described, a unique wind-tunnel test facility was constructed. This facility, specifically designed to test heat exchangers, is shown in Fig. 2. As seen there, it is made up of four separate legs and a test section. Each of the legs either delivers or extracts air to or from the test section.

The figure shows fresh air taken from the outdoors (Outside Stream) and delivered to the test section. This air passes through one side of the mass exchanger and emerges as the Supply Stream. Indoor air (Return Stream), enriched with water vapor and possibly contaminated by the addition of carbon dioxide ( $\text{CO}_2$ ) gas,

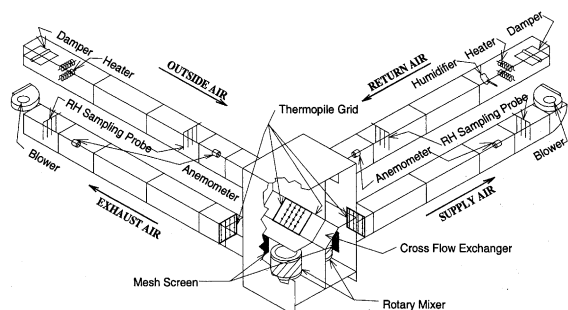


Fig. 2. Test facility.

is ducted to the other side of the mass exchanger from where it emerges as the Exhaust Stream. The latter is vented to the outdoors. In this configuration, water vapor passes from the Return Stream to the Supply Stream.

The ductwork that comprises each of the four legs is made of sheet metal that was meticulously sealed at all joints to prevent leaks. Each duct is 20 ft (6.1 m) long and has a rectangular cross-section of 10 by 12 in. (25.4 by 30.5 cm). The hydraulic diameter of these ducts is 0.909 ft (0.277 m), and the corresponding length-to-diameter ratio is approximately 22. This length/diameter ratio is the longest that could be accommodated in the physical space available. The motivation for using ductwork with the largest possible length/diameter ratio was to achieve fully developed and well-mixed flows at the four sites at which measurements were taken. Additional mixing was provided by the use of rotary mixers and screens situated downstream of the test section.

Considerable attention was given to the use of proper instrumentation. All instruments that were used during the experimental work were calibrated in situ. The quantities that were measured included:

1. humidity,
2. volumetric flowrate,
3. temperature,
4. pressure,
5. concentration of  $\text{CO}_2$ .

Aside from  $\text{CO}_2$ , all of these quantities were separately measured in each of the four respective airstreams. The  $\text{CO}_2$  measurements will be discussed in detail later.

The water vapor content in each of the four airstreams was characterized in terms of their respective humidity ratios. During the initial experimentation, commercially available relative humidity meters were used. It was soon found that the data collected using these meters were not internally consistent. To achieve the desired accuracy, it was found advantageous to design and fabricate special humidity-measuring devices based on the use of wet-bulb and dry-bulb thermocouples. Four identical humidity-measuring stations were fabricated. Each station consisted of a 1 1/2-inch

(3.8-cm) internal diameter PVC tube that is 2 ft (0.6 m) in length. Air drawn from a selected wind-tunnel cross-section is, in turn, drawn through the tube at velocities in the range from 800 to 1000 ft/min (4.06–5.08 m/s). These velocities were selected on the basis of information provided by Kuehn et al. [4] for the attainment of minimum-error humidity measurements. The tube wall was pierced by two holes situated 6 in. (15.2 cm) apart. A 30-gauge chromel–constantan thermocouple was threaded through each hole so that the junction was situated at the centerline of the tube. The downstream thermocouple was fitted with a woven-cotton wick. The wick was continuously fed with distilled water from a reservoir situated in the bottom wall of the tube just below the wet-bulb thermocouple. The eight thermocouples used in the four humidity measurement stations were individually calibrated to within  $0.1^\circ\text{F}$  ( $0.056^\circ\text{C}$ ) by means of an NIST-traceable mercury-in-glass thermometer.

The humid air that was processed by these humidity meters was drawn from the selected wind-tunnel sites that are identified in Fig. 2. At each of the measurement cross-sections, four sampling tubes were used as shown schematically in Fig. 3. Each tube was positioned perpendicular to one of the duct walls and extended across the duct cross-section. The tubes were made of 1/2-in. (1.27-cm) diameter PVC. In each tube, four 3/8-in. (0.95-cm) diameter holes were bored and oriented to face the oncoming airstream. All told, then, there were 16 sampling ports in each of the cross-sections at which the humidity was measured.

Volumetric flowrates were measured in each of the four legs of the test facility. The measurements were performed with vane anemometers that had been

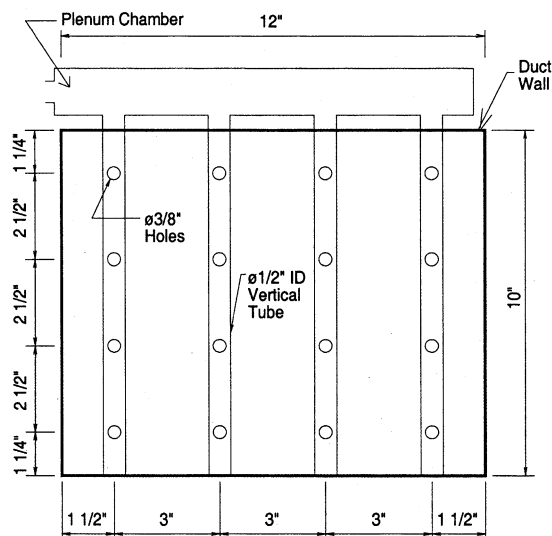


Fig. 3. Layout of the humidity sampling ports.

painstakingly calibrated in situ. For the calibration, the cross-section was subdivided into 99 measurement sites, and the local velocity at each site was determined by a hot-wire anemometer (which had a certified calibration accurate to within 1%). The thus-obtained velocity distributions were integrated across the section and thereby served as the volumetric-flow standard to which the respective vane anemometer was calibrated. This procedure was performed for all of the four vane anemometers used. The calibrations of the vane anemometers were performed over the entire range of flowrates employed during the course of the experiments.

The measured volumetric flowrates were converted to mass flowrates by use of the ideal gas law. For this purpose, thermocouples were installed to measure the temperatures at each of the locations where the volumetric flowrate was obtained. The thermocouples used for these measurements are the same as those situated in the humidity-measurement stations. In addition, static pressures were measured at the same locations. The static pressure measurements were facilitated by an MKS Baratron capacitance-type pressure meter capable of resolving  $10^{-4}$  mm Hg.

CO<sub>2</sub> was used to present a typical contaminant gas as suggested by Johnson [5]. In principle, it would have been desired to measure the concentrations of the CO<sub>2</sub> in each of the four legs of the test facility. However, the cost of the relevant instrumentation precluded purchase of the four needed concentration gauges. To facilitate the CO<sub>2</sub> determinations in the absence of complete instrumentation, it was assumed that a perfect mass balance for this species prevailed. That is, it was assumed that the sum of all inflows of CO<sub>2</sub> to the mass exchanger was precisely equal to the sum of all outflows. The concentrations of CO<sub>2</sub> were determined by means of a TSI CO<sub>2</sub> meter (Q-TRAK 8550) having a resolution of one part per million (ppm). This resolution was entirely adequate since the measured CO<sub>2</sub> concentrations were in the range of 300–900 ppm.

This CO<sub>2</sub> meter was used to measure three relevant concentrations:

1. in the airstream drawn from the outdoors,
2. in the airstream drawn from the laboratory room,
3. in the Supply Stream (downstream of the mass exchanger).

To create a mass transfer situation for CO<sub>2</sub>, a pressurized cylinder of the gas was connected to a tube through which CO<sub>2</sub> was delivered to the Return Stream via a set of four distribution tubes identical to those used in connection with the sampling of the humidities of the airstreams. This use of distribution tubes ensured that the CO<sub>2</sub> was uniformly delivered. For the metering of the delivered gas flow, a calibrated orifice was installed in the delivery system. The thus-enriched Return Stream

interacted with the less-rich Supply Stream through the walls of the mass exchanger. The extent of the mass transfer was identified by the measurement of the concentration of CO<sub>2</sub> in the Supply Stream.

#### 4. Operating protocol

As noted earlier, in connection with the description of the test facility, humidification equipment was installed just downstream of the entrance of the Return-Stream leg. Prior to the commencement of a water vapor transfer data run, the humidifier and the airflows were turned on and permitted to warm up to steady operating conditions. Generally, an hour was sufficient to achieve steady state. During the data acquisition, four independent sets of readings of each of the measured quantities were made. Approximately five minutes were allowed between the collection of each data set.

For the CO<sub>2</sub> data runs, the protocol was formulated to take account of the fact that a single concentration meter had to be used for three independent measurements. Prior to the initiation of the airflows in the test facility, the concentration of CO<sub>2</sub> in the laboratory was measured. Next, with the airflows established but before CO<sub>2</sub> was drawn from the pressurized tank, the concentration of CO<sub>2</sub> in the outside air was determined from measurements made in the Supply-Stream leg. This mode of determination of the outside-air CO<sub>2</sub> concentration was chosen to facilitate the use of the single available concentration meter. The errors associated with this measurement were calculated and found to be insignificant (no more than 5%). Then, after the delivery of CO<sub>2</sub> to the Return-Stream leg was initiated and maintained steady, the CO<sub>2</sub> concentration in the Supply-Stream leg was measured once again.

#### 5. Results and discussion

A broadly accepted measure of the performance of a heat exchanger is called the heat transfer effectiveness  $\varepsilon$ . It is, therefore, natural to characterize the performance of a mass exchanger by a similarly defined quantity  $\varepsilon_m$ , to be denoted as the mass transfer effectiveness for water vapor. The definition of  $\varepsilon_m$  is as follows:

$$\varepsilon_m = \frac{(\dot{m}_a)_{\text{RET/EXH}}[\omega_{\text{RET}} - \omega_{\text{EXH}}]}{(\dot{m}_a)_{\text{MIN}}[\omega_{\text{MAX}} - \omega_{\text{MIN}}]} = \frac{(\dot{m}_a)_{\text{OUT/SUP}}[\omega_{\text{SUP}} - \omega_{\text{OUT}}]}{(\dot{m}_a)_{\text{MIN}}[\omega_{\text{MAX}} - \omega_{\text{MIN}}]}, \quad (1)$$

where  $\dot{m}_a$  is the mass flowrate of air in either the Return/Exhaust circuit (RET/EXH) or the Outside/Supply circuit (OUT/SUP). In addition,  $\omega$  denotes the humidity ratio, respectively, in the Return Stream (RET), Exhaust

Steam (EXH), Supply Stream (SUP) or Outside Stream (OUT). The subscripts MIN and MAX are used to identify the smallest and largest of the respective quantities, humidity ratio and airflow. The interchangeability of the numerators in Eq. (1) is predicated on a perfect mass balance for the flow of water vapor in and out of the mass exchanger. In the present experiments, the water vapor mass balance was found to close to within 6%, on the average.

In the special case of matched air flowrates, which was fulfilled within 1.5% or better in the present experiments, Eq. (1) reduces to

$$\varepsilon_m = \frac{[\omega_{\text{RET}} - \omega_{\text{EXH}}]}{[\omega_{\text{MAX}} - \omega_{\text{MIN}}]} = \frac{[\omega_{\text{SUP}} - \omega_{\text{OUT}}]}{[\omega_{\text{MAX}} - \omega_{\text{MIN}}]}. \quad (2)$$

The measured experimental data were used in conjunction with Eq. (2) to evaluate mass transfer effectiveness. The corresponding results are shown as the square data symbols in Fig. 4. In this figure,  $\varepsilon_m$  is plotted against the Supply-Stream face velocity in standard feet per minute (SFPM). In particular, the velocity reported was determined by dividing the volumetric flow in standard cubic feet per minute (SCFM) by the open area of the face of the mass exchanger. As seen in the figure,  $\varepsilon_m$  for the velocity range of the experiment were of the order of 20%. Further inspection of the figure reveals that  $\varepsilon_m$  decreases with increasing velocity – a trend which is commonly encountered for the heat transfer effectiveness  $\varepsilon$ .

The measured effectiveness of 20% corresponds to a relatively high face velocity. To provide perspective for this effectiveness value, a simple model was devised for computing the  $\varepsilon_m$  for velocities other than those of the present experiments. To begin the discussion of the model, it is useful to make reference to the well-established relationship between the heat exchanger effectiveness  $\varepsilon$  and the NTU parameter, which is quoted here for convenience

$$\varepsilon = 1 - \exp[-\text{NTU}^{0.22} \{ \exp(-\text{NTU}^{0.78}) - 1 \}]. \quad (3)$$

This equation applies to a cross-flow situation in which both of the participating fluids are channeled (alternatively referred to as unmixed). In addition, the general form of Eq. (3) has been specialized to the case in which both streams have the same value of the capacity rate  $\dot{m}c_p$ . The quantity NTU which appears in Eq. (3) is defined as:

$$\text{NTU} = \frac{UA}{(\dot{m}c_p)_{\text{MIN}}} = \frac{1}{R(\dot{m}c_p)_{\text{MIN}}}, \quad (4)$$

where  $U$  represents the overall heat transfer coefficient and  $A$  is the corresponding surface area for heat transfer. The quantity,  $(\dot{m}c_p)_{\text{MIN}}$ , is the capacity rate for the lesser of the two participating fluid flows. Inasmuch as the product  $UA$  is precisely equal to the overall thermal resistance  $R$ , the second form of Eq. (4) is also appropriate. To adapt Eqs. (3) and (4) for mass transfer, a few notational changes are needed. The first change is to replace  $\varepsilon$  by  $\varepsilon_m$  and  $(\dot{m}c_p)_{\text{MIN}}$  by  $(\dot{m}_a)_{\text{MIN}}$ . The appropriateness of this change is readily verified by examination of the defining equation for  $\varepsilon_m$ , Eq. (1). As seen there, the factor that multiplies the change in the transferred quantity  $\omega$  is  $(\dot{m}_a)_{\text{MIN}}$ . In the corresponding definition of the heat transfer effectiveness  $\varepsilon$ ,  $(\dot{m}c_p)_{\text{MIN}}$  is the factor that multiplies the transferred quantity  $T$  (temperature).

The second modification relates to transforming the thermal resistance  $R$  in Eq. (4) to the mass transfer resistance  $R_m$ . In common with the thermal resistance, the mass transfer resistance also consists of three terms:

1. the convective resistance to mass transfer at one face of the permeable wall  $R_1$ ,
2. the diffusive resistance for the movement of mass within the membrane wall  $R_d$ ,
3. the convective resistance to mass transfer at the other face of the membrane wall  $R_2$ .

When these changes are incorporated into Eqs. (3) and (4), the resulting mass transfer forms emerge as:

$$\varepsilon = 1 - \exp[-\text{NTU}_m^{0.22} \{ \exp(-\text{NTU}_m^{0.78}) - 1 \}], \quad (5)$$

and

$$\text{NTU}_m = \frac{1}{R_m(\dot{m}_a)_{\text{MIN}}}. \quad (6)$$

It is well established from the underlying theories of convective heat and mass transfer that the two transfer processes are analogous. For laminar flow, the analogy between heat and mass transfer is precise. The practical outcome of the analogy is that a Nusselt–Reynolds–Prandtl relationship transforms without change to a Sherwood–Reynolds–Schmidt relationship. It is, therefore, easy to determine mass transfer coefficients (anal-

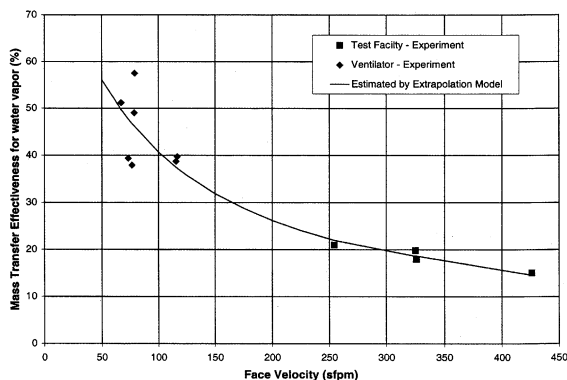


Fig. 4. Experimentally determined and extrapolated predictions of the mass transfer effectiveness for water vapor transfer.

ogous to heat transfer coefficients) provided that information already exists in the heat transfer literature for the geometry of interest. In the special case of laminar flow in ducts, the Nusselt number is independent of both the Reynolds number and the Prandtl number. By the same token, the Sherwood number is independent of both the Reynolds and the Schmidt numbers. As a consequence, mass transfer coefficients determined at a particular laminar Reynolds number are applicable at all other laminar Reynolds numbers.

From the theory of diffusive mass transfer in a permeable medium in which there is no convective motion, the resistance to diffusion is independent of the Reynolds numbers of the streams adjacent to the surfaces of the medium. Therefore, values of the mass transfer resistance of the wall  $R_d$  which are somehow obtained for laminar flows in the adjacent fluid streams can be used for other laminar Reynolds numbers in those streams. In the experimental work performed here, all of the investigated cases corresponded to laminar flow in the participating airstreams. Since all of the three mass transfer resistances  $R_1$ ,  $R_d$ , and  $R_2$  are independent of the Reynolds numbers, it follows that the total mass transfer resistance is also independent of the Reynolds numbers.

From the already discussed experimental results in Fig. 4 and using the definitions set forth in Eqs. (5) and (6) and the related text, the average numerical value of the total mass transfer resistance  $R_m$  was determined. Then, with this value of  $R_m$  as input, mass transfer effectivenesses were calculated from Eqs. (5) and (6) for a range of face velocities that extended well beyond those of the data points collected using the test facility. The thus-obtained variation of  $\epsilon_m$  with the face velocity is shown as the solid line in Fig. 4.

To test the validity of the extrapolation embodied in the just-displayed curve, a special experiment was set up and carried out. A commercially available housing for a residential ventilation unit was purchased and adapted to accommodate the mass exchanger that had formerly been in place in the test facility. Slight modifications were made in the housing in order to have a perfect fit of the exchanger therein. The housing contained blowers that were adequate for providing airflow to the exchanger. The cabinet of the housing was pierced by four 6-in. (15.2-cm) diameter circular ports. Each port was connected to a circular duct having a length-diameter ratio of 20. The four circular ducts corresponded functionally to the four legs of the test facility. The circular duct that corresponded to the Return-Stream leg was fitted with a heating element and a source of humidity.

This setup was regarded as a *field test*, and appropriately simple instrumentation was used. For example, to determine the relative humidity at strategic locations in the four circular ducts, a wand-type relative humidity probe (TSI Velocicalc, 8386) with a built-in temperature sensor was used. The humidity sensor was positioned in

the neighborhood of the centerline of the respective cross-sections. In addition, the pressures at these strategic locations were known. With this information, the values of the humidity ratio  $\omega$  were readily determined. The very same wand-type probe was capable of measuring the velocity at the centerlines of the respective circular ducts at the aforementioned strategic locations. With the centerline velocity known, it is possible to determine the mean velocity using the information provided by Schlichting [6], and from this, the volumetric flow and the mass flow both were readily calculated.

The knowledge of the humidity ratios and the mass flowrates enabled the mass transfer effectiveness  $\epsilon_m$  values to be determined. The results thus obtained are plotted as the diamond data symbols in Fig. 4. Although the data showed expected scatter, it is clear that they are strongly supportive of the extrapolated prediction (solid line) based on the test-facility data. This excellent agreement lends support to both sets of data and the methodology used for the extrapolation.

Furthermore, it is especially noteworthy that the effectiveness values for the range of velocities used in the simulated field test fall in the approximate range of 50%. Effectiveness values of this level are indicative of satisfactory performance. Indeed, this effectiveness appears to be especially favorable in light of the fact that the streamwise length of the heat exchanger was of the order of one foot. It is a certainty that higher effectivenesses would have resulted had a longer streamwise length been used. In light of these results, it would appear that mass exchangers having walls made of the composite permeable material used here are potentially viable commercial products.

The data scatter for the simulated field test is quite appropriate. In a field test, less detailed measurements are generally made relative to the more localized measurements that are common in laboratory work. It is the opinion of the authors that the scatter is entirely due to the coarse nature of the measurements.

A second focus of this investigation was to determine the selectivity of the composite permeable membrane from which the walls of the mass exchanger were fabricated. Selectivity is a property which relates to the different capabilities of the membrane to pass various gases through it. For the application considered here, the most desired property of the membrane is to pass water vapor at a high rate. From the standpoint of indoor air quality, it would be desired that the membrane would pass virtually no other gaseous species. In the experiments that were performed here,  $\text{CO}_2$  was selected to be representative of a gas whose passage through the membrane is to be blocked.

The experimental methodology relevant to  $\text{CO}_2$  has already been discussed in detail. In recognition of the fact that the  $\text{CO}_2$  concentration was measured in terms of the mole fraction  $y$ , the mass transfer effectiveness for

the case of matched airflows on the two sides of the exchanger reduces to

$$(\varepsilon_m)_{\text{CO}_2} = \frac{[Y_{\text{SUP}} - Y_{\text{OUT}}]}{[Y_{\text{MAX}} - Y_{\text{MIN}}]} \quad (7)$$

All of the mole fractions that appear in Eq. (7) were determined as part of the experimental work. Two independent experiments were made to determine the mass transfer effectiveness for CO<sub>2</sub>. These experiments were performed for face velocities of 300 sfpm (1.52 m/s). The corresponding effectiveness values were 0.34% and 1.01%. The extreme smallness of these values provides strong testimony to the excellent blocking capability of the present composite membrane for CO<sub>2</sub> transfer.

To characterize the selectivity  $S$ , it is common to evaluate the ratio:

$$S = \frac{\varepsilon_m}{(\varepsilon_m)_{\text{CO}_2}}, \quad (8)$$

where the numerator refers to water vapor transfer and the denominator refers to CO<sub>2</sub> transfer. Both numerator and denominator have to be evaluated at the same face velocities which, for the present situation, correspond to 300 sfpm (1.52 m/s). The  $S$  values determined here are 61 and 21, respectively. Although these values are widely scattered, they provide strong testimony to the excellent selectivity of the present composite permeable membrane. It has been shown by Johnson (1997) that the selectivity of a composite membrane for CO<sub>2</sub> is similar in magnitude to those for other gases such as formaldehyde, sulfur hexafluoride, and propane.

## 6. Concluding remarks

It has been demonstrated by qualitative experiments that it is possible to use a polymer-based composite permeable membrane to fabricate a highly effective mass exchanger which transfers water vapor with a high degree of effectiveness while inhibiting the transfer of other gaseous species. The membrane consisted of an extremely thin, continuous polymer layer atop an ordinary, commercially available polymer. The thin polymer layer is hydrophilic and dissolves water vapor that contacts its surface. The water is transferred across the polymer by solution diffusion. Other gases which are insoluble in the polymer layer cannot pass through. It was also demonstrated that the composite membrane could be fashioned into modules and then stacked to form a cross-flow mass exchanger. Experiments were performed to determine the transfer characteristics of both water vapor and carbon dioxide.

The experiments for water vapor were performed in two parts. The first set of experiments utilized a special wind-tunnel test facility that was precisely instrumented.

In contrast, the second set of experiments was carried out to simulate a field test. The experimental data from the wind-tunnel tests were used to evaluate the total resistance of the composite membrane for mass transfer. This resistance value was then employed to develop an extrapolation model to predict the results that were measured during the simulated field test. The agreement between the extrapolated predictions and the measured field-test results was excellent. It was found that mass transfer effectivenesses for water vapor in the range of 50% were obtainable.

In addition to the experiments involving water vapor, independent experiments employing carbon dioxide as the mass transfer species were performed. The experimental results demonstrated that the composite permeable membrane was virtually impassable to carbon dioxide. To obtain a quantitative measure of the selectivity of the membrane to species other than water vapor, a parameter consisting of the ratio of the effectiveness for water vapor transfer to the effectiveness for carbon dioxide transfer was utilized. The values of the selectivity parameter ranged from 21 to 61.

The present work demonstrated conclusively that highly effective mass exchangers can be based on the use of composite polymer membranes as the exchanger walls. Effectivenesses for water vapor transfer as high as 50% were determined. This level of effectiveness can be regarded as highly satisfactory from the standpoint of practical application. The degree of selectivity was also found to be high enough so that mass exchangers based on the present composite membrane can be used in applications where indoor air quality is of primary importance.

## Acknowledgements

The authors gratefully acknowledge the support of the National Science Foundation under grant 9801062.

## References

- [1] W.J. Fisk, K.M. Archer, F.J. Offermann, R.E. Chant, D. Hekman, B.S. Pederson, Performance of residential air-to-air heat exchangers during operation with freezing and periodic defrost, ASHRAE Transactions, Part 1B 91 (1985).
- [2] W.J. Fisk, B.S. Pederson, D. Hekman, R.E. Chant, H. Kaboli, Formaldehyde and tracer gas transfer between airstreams in enthalpy-type air-to-air heat exchangers, ASHRAE Transactions, Part 1B 91 (1985).
- [3] C.G. Barringer, C.A. McGugan, Effect of residential air-to-air heat and moisture exchangers on indoor humidity, ASHRAE Transactions, Part 1 94 (1989).



- [4] T. Kuehn, J. Ramsey, J.L. Threlkeld, *Thermal Environmental Engineering*, third ed., Prentice-Hall, Upper Saddle River, NJ, 1998.
- [5] J.E. Johnson, *Heat and mass transfer between two fluid systems separated by a thin, permeable barrier*, Ph.D. Thesis, Department of Mechanical Engineering, University of Minnesota, Minneapolis, MN, 1997.
- [6] H. Schlichting, *Boundary Layer Theory*, seventh ed., McGraw-Hill, New York, NY, 1979.